Supplementary Information (SI)

Exploring the potential of a potassium 4-piperidinolate/4-pyridinolate pair for reversible hydrogen storage

Alexis Munyentwali [a,b], Yang Yu [a,b], Khai Chen Tan [a,b], Qijun Pei [a,b], Zhaoji Huang [c], Anan Wu [c,*], Teng He [a,b,d*], Ping Chen [a,b,d]

[a] *Dalian Institute of Chemical Physics, Chinese Academy of Sciences, Dalian 116023, China*

[b] *Center of Materials Science and Optoelectronics Engineering, University of Chinese Academy of Sciences, Beijing 100049, China*

[c] *Fujian Provincial Key Laboratory of Theoretical and Computational Chemistry, College of Chemistry and Chemical Engineering, Xiamen University, Xiamen, 361005, China*

[d] *State Key Laboratory of Catalysis, Dalian Institute of Chemical Physics, Chinese Academy of Sciences, Dalian 116023, China.*

* *Corresponding authors.*

E-mail addresses: ananwu@xmu.edu.cn (A. Wu), heteng@dicp.ac.cn (T. He)

1. DFT calculations

Enthalpy changes of dehydrogenation (ΔH_d), HOMO and LUMO energy levels, and bond lengths were calculated using X1s, which is a DFT-based method that combines *B3LYP* with neural network correction. As an additional descriptor, the method also includes a spin change from molecules to atoms during atomization[1]. All the calculations were carried out using the Gaussian 16 package[2].

2. Experimental sections

2.1. Materials and synthesis

4-hydroxypyridine (97%, Thermo Scientific), 4-hydroxypiperidine (98%, Acmec Biochemical), potassium hydride (95%, Aldrich), potassium hydroxide (99.99%, Innochem), cyclohexanol (99%, Alfa Aesar), potassium phenoxide (99.87%, Alfa Aesar), and sodium hydride (95%, Aldrich) were utilized without further purification. Commercial catalysts 5% Rh/C (Acmec Biochemical), 5% Rh/Al_2O_3 (Sigma Aldrich), 5% Pd/C (Alfa Aesar), 5% Pt/C (Alfa Aesar), and 5% Ru/Al_2O_3 (Sigma Aldrich) were reduced under H_2 atmosphere with a flow rate of 30 mL min^{-1} at 250 °C for 2 h before use.

Synthesis of potassium 4-piperidinolate (4-K-pip)

4-K-pip was synthesized by reacting 4-hydroxypiperidine with potassium hydride. In a typical synthesis, 0.01 mol of 4-hydroxypiperidine and 0.01 mol of potassium hydride, together with 30 mL of tetrahydrofuran (THF) solvent, were loaded into a Parr 550 stainless steel autoclave (100 mL), which was then tightly sealed under an argon atmosphere inside a glove box. This air-tight autoclave was removed from the glove box and then connected to a workstation equipped with a

system for continuous monitoring and control of stirring speed, temperature, and pressure. The reaction was conducted at 90 °C with a stirring speed of 500 rpm. During this synthesis, approximately one equivalent of H_2 gas was released, indicating the formation of 4-K-pip as per the chemical equation depicted in the **Scheme. S1**. After the reaction completion, the liquid mixture was transferred into a volumetric flask equipped with a closed glass adapter inside the glove box. A solid sample of 4-K-pip was obtained after evaporating THF at 38 °C using a rotary evaporator under vacuum conditions. Potassium cyclohexanolate (K-cycloh) and sodium 4-piperidinolate (4-Na-pip) were synthesized using the same method.

Synthesis of potassium 4-pyridinolate (4-K-pyr) through ball milling

0.01 mol of 4-hydroxypyridine and 0.01 mol of potassium hydride were loaded into a 180 mL tungsten carbide ball mill vessel with a ball-to-sample mass ratio of 100:1 under an argon atmosphere inside a glove box. The vessel was then tightly closed, and the mixture was ball milled for 8 h at 200 rpm using a RETSCH centrifugal ball mill S100. Afterwards, heating the resulting mixture at 120 °C generated approximately one equivalent of H_2, indicating the formation of 4-K-pyr, as illustrated by the chemical equation in **Scheme S1.**

Synthesis of potassium 4-pyridinolate (4-K-pyr) in aqueous solution

0.01 mol of 4-hydroxypyridine and 0.01 mol of potassium hydroxide were dissolved in 30 mL of deionized water and then mixed altogether in a 100 mL flask for 5 h at room temperature. A solid sample of 4-K-pyr was obtained after evaporating the water using a rotary evaporator. The sample was further dried at 200 °C for 5 h under vacuum conditions.

2.2. Materials characterization and crystal structures

Liquid state ^{1}H and ^{13}C NMR characterizations were conducted using a JEOL JNM-ECZL (400 MHz) NMR spectrometer at ambient temperature. Powder X-ray diffraction (PXRD) measurements were performed on a PANalytical X'pert diffractometer with Cu-Ka radiation (λ= 0.154 nm) at 40 kV and 40 mA. Samples were tested in a stainless-steel sample holder covered with Kapton to avoid contamination. The laboratory powder XRD pattern of potassium 4-pyridinolate (4-K-pyr) can be indexed into an orthorhombic structure with space group *Pnma* (No.62). The crystal structure of 4-K-pyr was solved using direct space methods combined with the first-principles molecular dynamics simulated annealing with the optimized $C_5H_4NO^-$ configuration. Rietveld structural refinement on the optimal structural candidate was performed using the GSAS package on the XRD data[3]. Due to the insensitivity of XRD to the lightweight elements and the inadequate number of lab PXRD observations, the $C_5H_4NO^-$ anion was kept as a rigid body during the refinement. The $C_5H_4NO^-$ rigid body, potassium positions, and lattice parameters were refined, yielding the agreement factors of R_{wp}=0.1001, R_p=0.0724, and χ^2=3.83. Rietveld fits to the XRD patterns of KOC_5H_4N is shown in **Fig. S5**. Crystallographic details can be found in the CIF file deposited in the Cambridge Structural Database (CSD) under deposition number CCDC 2450241.

2.3. NMR data

Potassium 4-piperidinolate: ^{1}H NMR (400 MHz, DMSO-d6, 25°C, TMS). δ 3.37 (1H, m), 2.79 (2H, d, *J*=12.0), 2.35 (2H, td, *J*=11.8, 2.0), 1.54 (2H, d, *J*=9.8), 0.99 ppm (2H, ddd, *J*=18.1, 11.7, 6.1). ^{13}C NMR (400 MHz, DMSO-d6, 25°C, TMS). δ 71.69, 46.21, 43.09 ppm.

Potassium 4-pyridinolate: ^{1}H NMR (400 MHz, DMSO-d6, 25°C, TMS). δ 7.54 (2H, dd, *J* = 5.1, 1.3 Hz), 5.86 ppm (2H, dd, *J* = 5.0, 1.4 Hz). ^{13}C NMR (400 MHz, DMSO-d6, 25°C, TMS). δ 176.22, 149.45, 117.16 ppm.

Potassium cyclohexanolate: ^{1}H NMR (400 MHz, DMSO-d6, 25°C, TMS). δ 3.32 (1H, dd, *J* = 10.9, 7.5 Hz), 1.59 (4H, dd, *J* = 22.4, 8.4 Hz), 1.42 (1H, d, *J* = 11.9 Hz), 1.13 (2H, dd, *J* = 24.0, 12.0 Hz), 0.97 ppm (2H, m).

Sodium 4-piperidinolate: ^{1}H NMR (400 MHz, DMSO-d6, 25°C, TMS). δ 3.41 (1H, m), 2.79 (2H, d, *J* = 12.0 Hz), 2.36 (2H, td, *J* = 11.8, 1.9 Hz), 1.53 (2H, d, *J* = 9.6 Hz), 0.90 ppm (2H, qd, *J* = 12.1, 3.7 Hz). ^{13}C NMR (400 MHz, DMSO-d6, 25°C, TMS). δ 37.1, 44.8, 67.8 ppm.

2.4. Temperature-programmed desorption analysis

Thermal decomposition analysis of 4-K-pip mixed with the 5% Rh/C catalyst was conducted using a temperature-programmed desorption system coupled with a mass spectrometer, TPD-MS (HPR20-Hiden), to determine the temperature range of H_2 release. In this analysis, a 25-30 mg mixture of the 4-K-pip with the catalyst (substrate-to-Rh molar ratio of 5:1) was loaded into an air-tight TPD-MS reactor sample holder under an argon atmosphere inside a glove box. The analysis was conducted from room temperature to 200 °C, at a 2 °C/min heating rate under 20 mL/min argon flow.

2.5. Hydrogen absorption and desorption in the solid state

Hydrogen absorption and desorption tests were conducted using a homemade HPSA-auto Pro gas adsorption analyzer (TJTECH, China), operated automatically by GAD-analysis software. Before any test, the volume calibration of a loaded sample chamber was performed in three cycles. In a typical H_2 absorption/desorption test, 150-200 mg of a sample (substrate-to-metal molar ratio of 2:1 for H_2 absorption, and 5:1 for H_2 desorption) was ground using a mortar and pestle under an argon atmosphere inside a glove box. However, to ensure intimate contact between the reactant and catalyst, this mixing process was conducted in three rounds of a 5-minute grinding step for every sample preparation. After each grinding round, the powder was scraped off the mortar walls using a spatula before starting the next round. The well-mixed sample was recovered and loaded into a stainless-steel sample chamber of the HPSA-auto Pro gas adsorption analyzer, which was then tightly closed to prevent any gas leakage during the test. After volume calibration, H_2 desorption was carried out from room temperature to 120 °C at a heating rate of 2 °C/min under vacuum (0.01 bar). On the other hand, volume calibration for the H_2 absorption process was carried out at the reaction temperature (120 °C), after heating the sample chamber from room temperature at a heating rate of 2 °C/min. H_2 absorption tests were carried out using a pressure of 60 bar. The H_2 absorption and desorption data were generated by the GAD-analysis software of the HPSA-auto Pro gas adsorption analyzer. After the completion of each test, the solid sample was recovered, dissolved in an appropriate deuterated solvent, and then filtered for characterization and determination of the conversion percentage using ^{1}H NMR spectroscopy.

2.6. Hydrogenation and dehydrogenation experiments in aqueous solution

The synthesis and hydrogenation of 4-K-pyr in an aqueous solution were carried out in one-pot mode using a 100 mL Parr stainless steel batch reactor (autoclave) equipped with a system for continuous monitoring and control of stirring speed, temperature, and pressure. In a typical experiment, the autoclave was loaded with 2 mmol of 4-H-pyr and potassium hydroxide in a slight excess (molar ratio 1:1.1) to ensure complete conversion and to keep the solution alkaline. 30 mL of deionized water was added, and the reaction was run for 5 h at room temperature with a stirring speed of 500 rpm. After this synthesis step, a hydrogenation catalyst was added into the autoclave in a substrate-to-metal molar ratio of 30:1. The reactor was sealed, purged with argon 5 times to remove air, and then heated to the reaction temperature before charging it with a desired H_2 pressure. The progress of the hydrogenation reaction was monitored through the pressure change in the reactor, and a final solution sample was characterized by using ^{1}H and ^{13}C NMR spectroscopy.

Catalytic dehydrogenation experiments in aqueous solution were conducted outside the glove box under water reflux, using an oil bath as the heating system. However, deaerated water was utilized as a solvent, and all sample preparations were conducted inside an argon-filled glove box to protect the reduced catalysts from being deactivated by oxygen. Besides, KOH was added to the reaction system to keep the solution alkaline and prevent any possible hydrolysis of the metal-containing hydrogen-rich compounds into their hydroxide precursors. In a typical experiment, 2 mmol of H-rich substrate, 5 mmol of KOH, and a catalyst (substrate-to-metal molar ratio of 20:1) were loaded into a 100 mL three-neck round-bottomed flask containing a magnetic stir bar inside an argon-filled glove box. After closing the three openings of the flask

with a condenser, glass adapter, and a rubber septum, the flask was taken outside the glove box and placed into an oil bath. Then, 25 mL of deaerated water was added into the flask through the rubber septum using a long syringe under an argon flow for 5 min. Afterwards, the reaction mixture was heated to 100 °C as the target temperature. Small aliquots were taken from the reaction mixture at various times using a syringe via the rubber septum for qualitative and quantitative analyses using ^{1}H and ^{13}C NMR spectroscopy.

2.7. Hydrogenation and dehydrogenation cycles in aqueous solution

The hydrogenation process of every cycle was conducted in a 100 mL Parr stainless steel batch reactor (autoclave) equipped with a system for continuous monitoring and control of stirring speed, temperature, and pressure. In the hydrogenation process of the first cycle, 4 mmol of potassium 4-pyridinolate (4-K-pyr) and 8 mmol of KOH were dissolved in 30 mL of deaerated water, followed by the addition of 5% Rh/C (4-K-pyr/Rh molar ratio: 20/1). This loaded autoclave was tightly sealed, purged with argon 5 times to remove air, and then heated to 100 °C before charging it with 40 bar H_2 as the hydrogenation pressure. After completion of the reaction, the autoclave was cooled to room temperature before venting the remaining H_2 pressure. Subsequently, a small sample of the final solution was taken for qualitative and quantitative characterization using ^{1}H and ^{13}C NMR spectroscopy. For the hydrogenation process of the subsequent cycles, a mixture recovered from the dehydrogenation flask was transferred into the hydrogenation autoclave. Then, the same procedure used during the first cycle was repeated.

Conversely, the dehydrogenation process for each cycle was carried out by transferring the reaction mixture from the hydrogenation reactor into a 100 mL three-neck round-bottomed flask

equipped with a condenser and then by following the procedure described in section 2.6. The reaction was run for 16 h at 100 °C under reflux.

3. Results

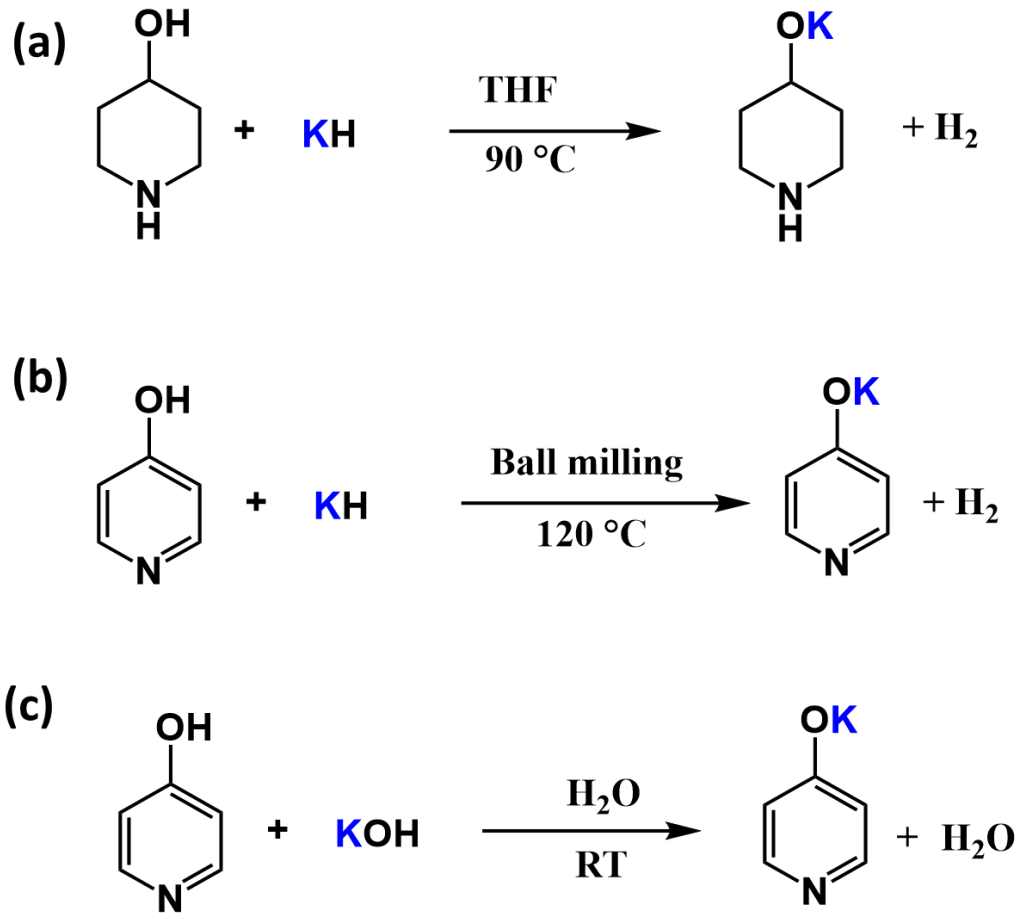

Scheme S1. (a) Synthesis of potassium 4-piperidinolate (4-K-pip). (b) Synthesis of potassium 4-pyridinolate (4-K-pyr) through ball milling. (c) Synthesis of 4-K-pyr in aqueous solution

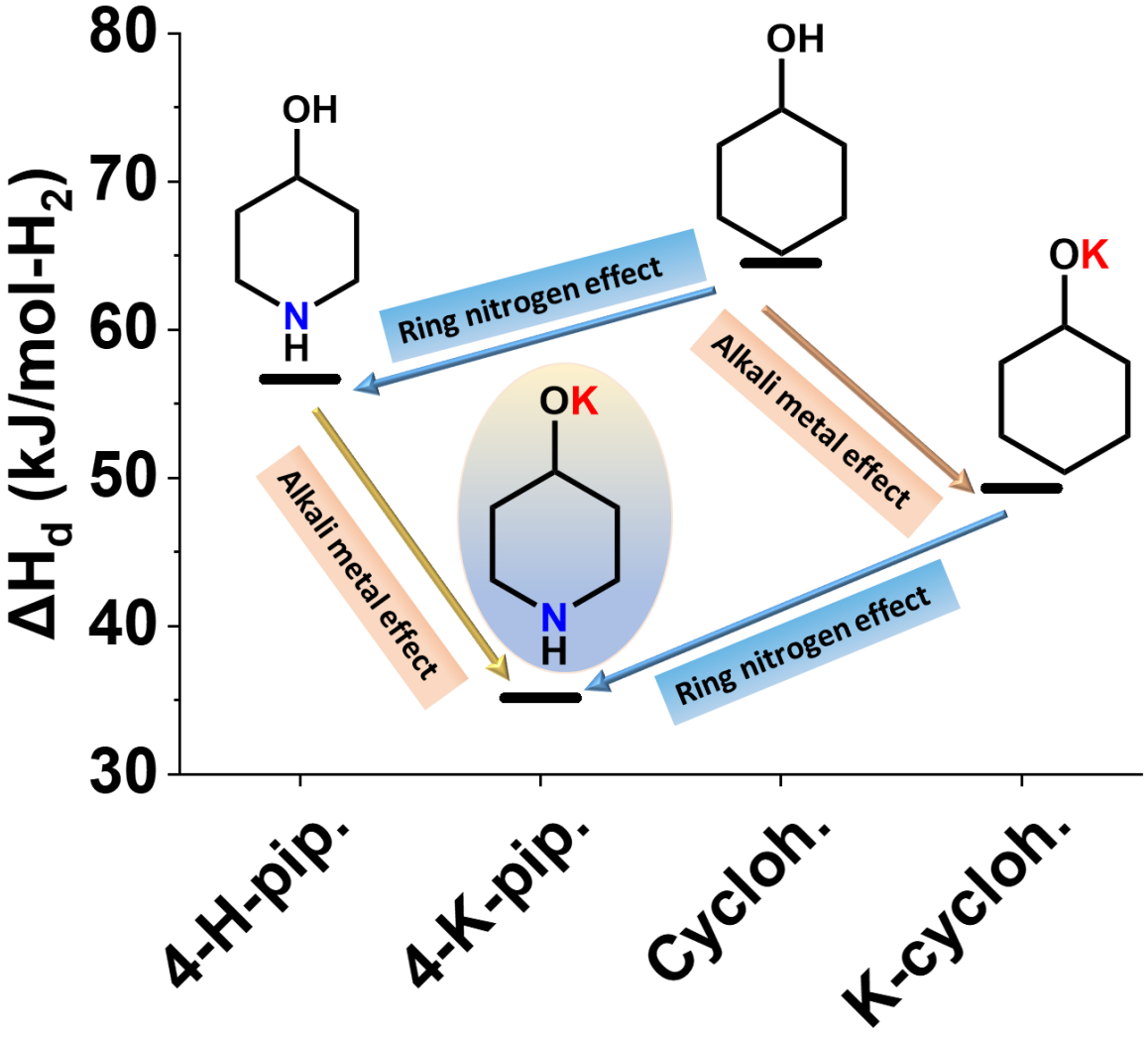

Fig. S1. A molecular engineering strategy that combines ring nitrogen and alkali metal effects within a single molecule to optimize the enthalpy change of dehydrogenation (ΔH_d).

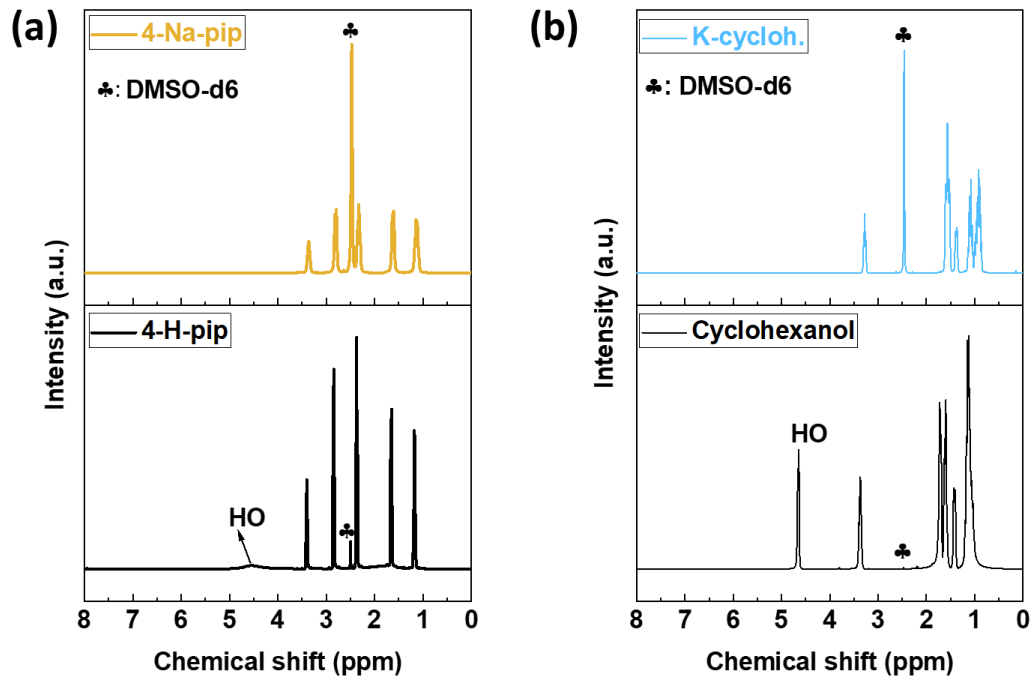

Fig. S2. (a) ^{1}H NMR spectrum of sodium 4-piperidinolate (4-Na-pip) compared to that of 4-hydroxypiperidine (4-H-pip). (b) ^{1}H NMR spectrum of potassium cyclohexanolate (K-cycloh) compared to that of cyclohexanol.

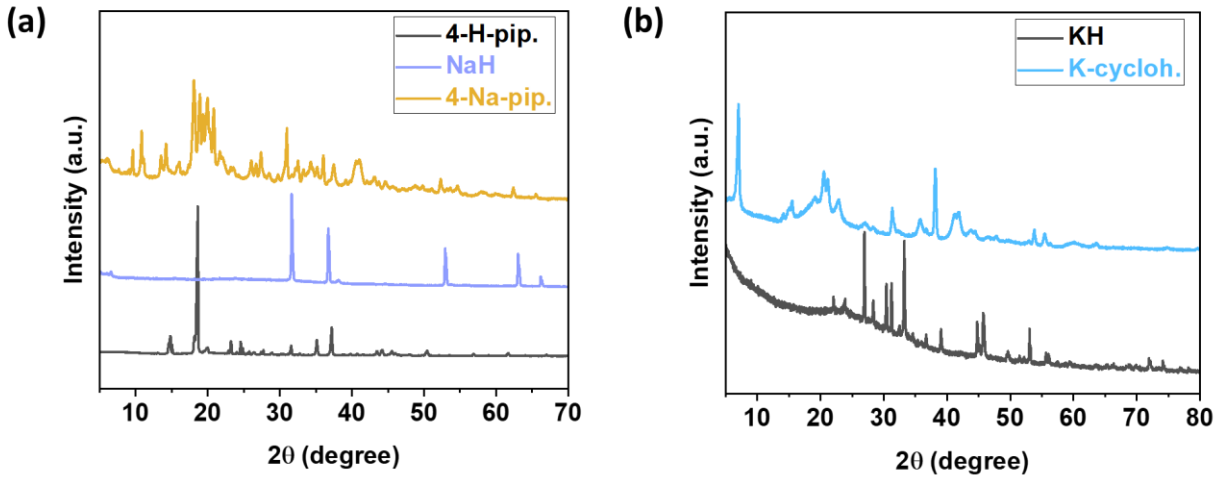

Fig. S3. (a) XRD pattern of sodium 4-piperidinolate (4-Na-pip) compared to those of 4-hyroxypiperidine (4-H-pip) and sodium hydride (NaH). (b) XRD pattern of potassium cyclohexanolate (K-cycloh) compared to that of potassium hydride.

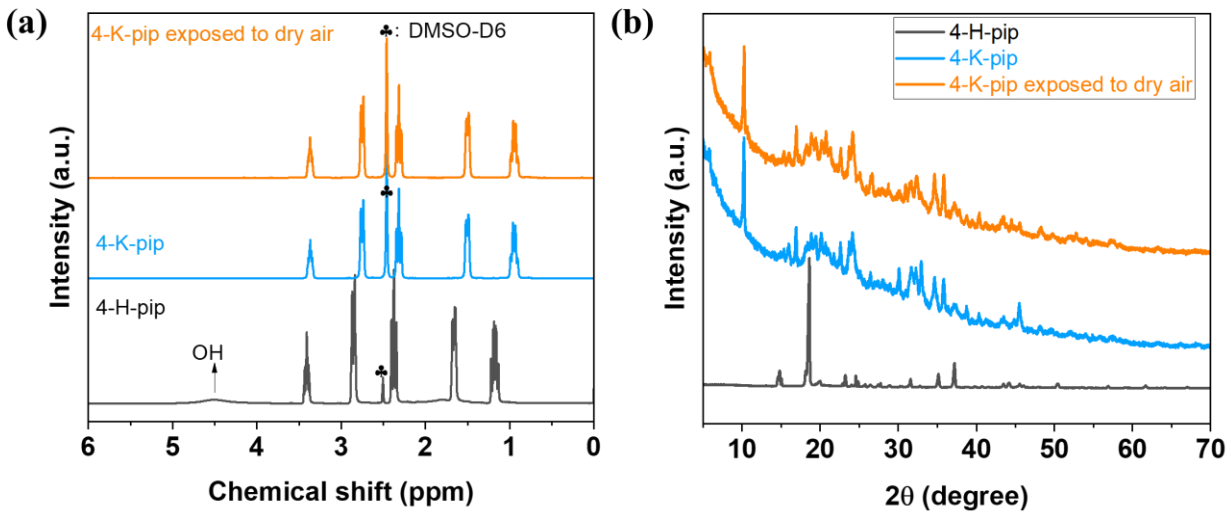

Fig. S4. Evidence of 4-K-pip stability in dry air. (a) ^{1}H NMR spectrum of a high-purity 4-K-pip sample exposed to dry air compared to those of the fresh sample kept under an inert atmosphere and the precursor material (4-H-pip). (b) PXRD pattern of a high-purity 4-K-pip sample exposed to dry air compared to those of the fresh sample kept under an inert atmosphere and the precursor material (4-H-pip). A high-purity 4-K-pip sample was synthesized by using a slight deficiency of KH compared to 4-H-pip to avoid any presence of KH in the final product. The as-synthesized material was then refined through heat treatment at 120 °C under vacuum to remove unreacted 4-H-pip, which has boiling and melting points of 95 °C and 115 °C, respectively.

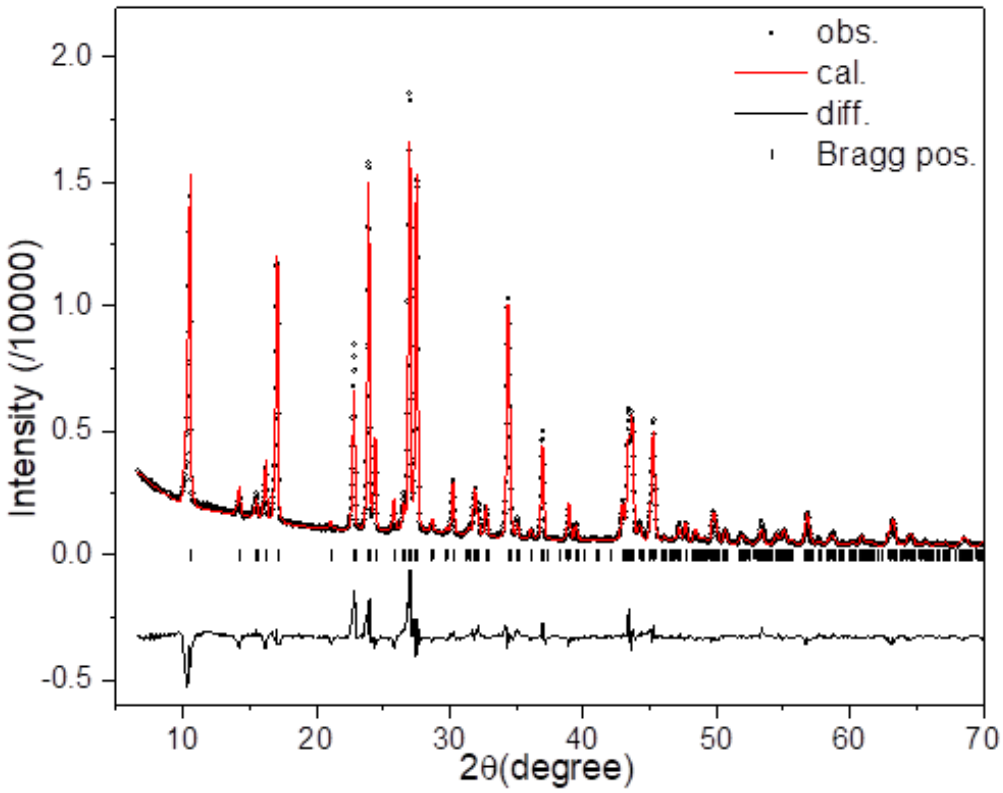

Fig. S5. The Rietveld fit to the XRD pattern of 4-K-pyr at 298 K. Experimental (circles), fitted (line), and difference (line below observed and calculated patterns). Vertical bars indicate the calculated positions of Bragg peaks. The goodness-of-fit factors are R_{wp}=0.1001, R_p=0.0724, and χ^2=3.83.

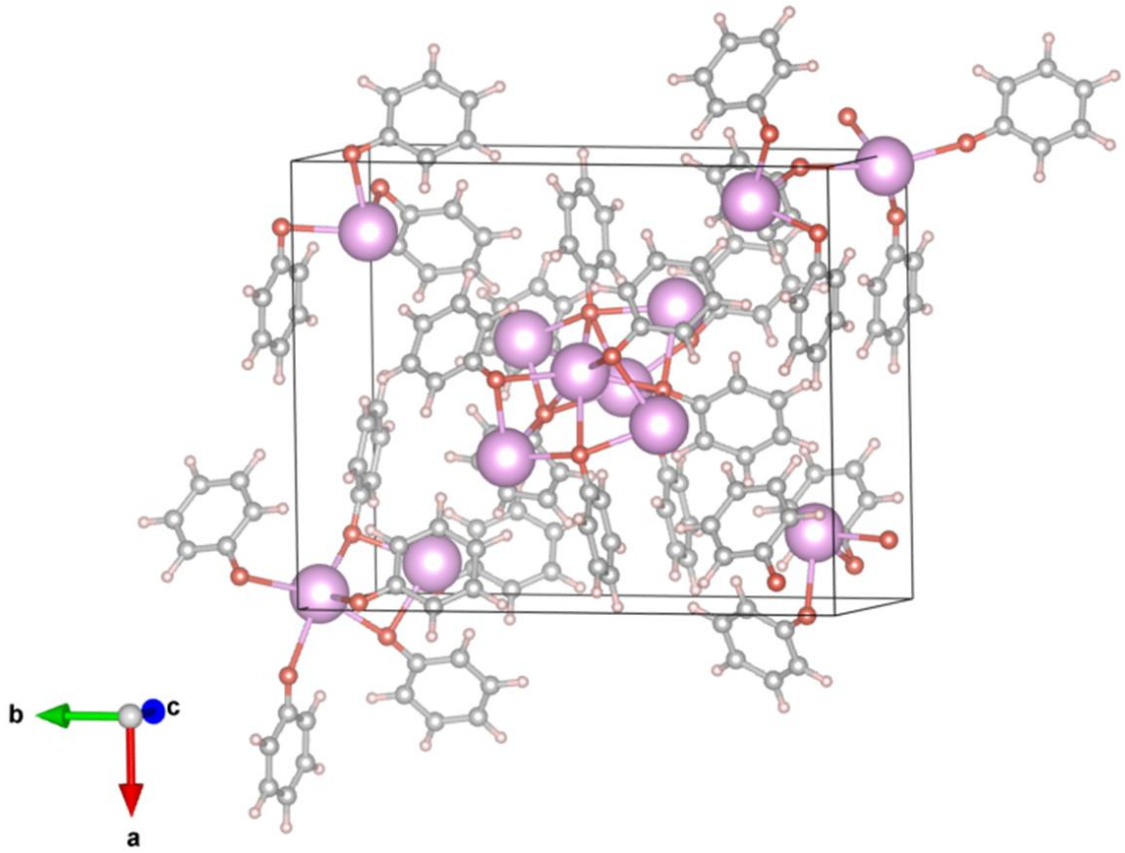

Fig. S6. The crystal structure of potassium phenoxide. Pink balls: K, red balls: O, grey balls: C, tan balls: H atoms[4].

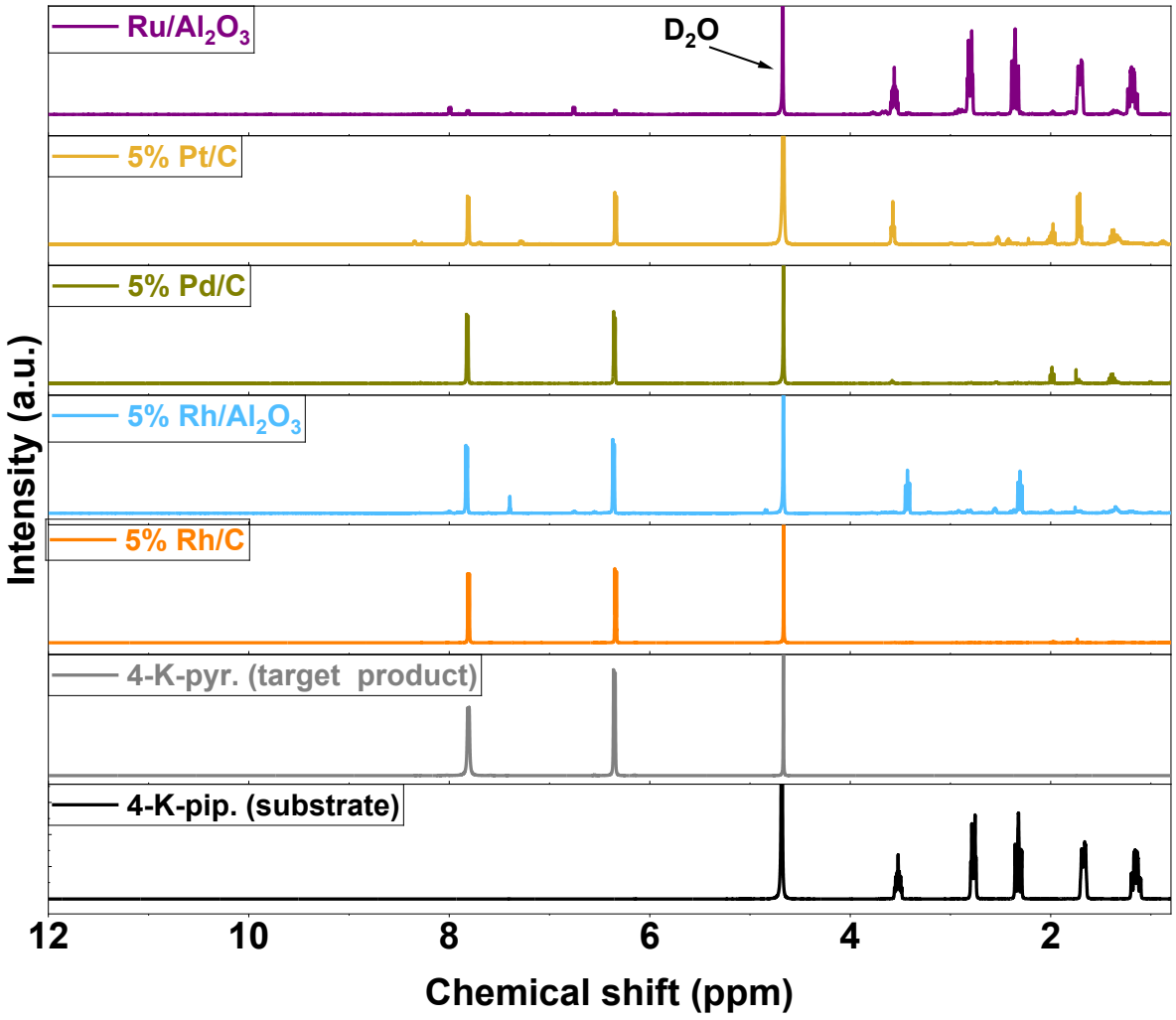

Fig. S7. ^{1}H NMR spectra of 4-K-pip post H_2 desorption samples using different metal-supported catalysts. These spectra are compared to those of the substrate and the target product to demonstrate the reaction conversion and selectivity.

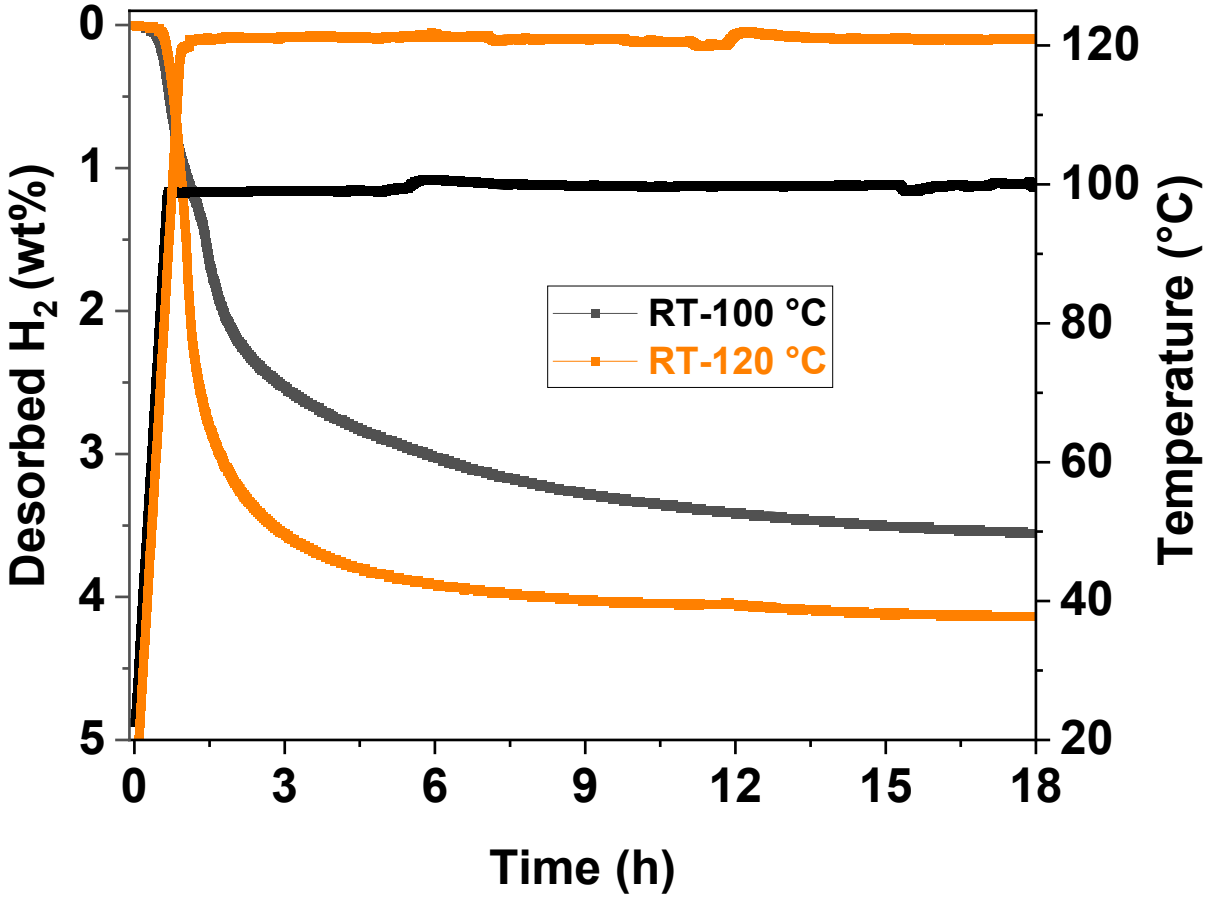

Fig. S8. Comparison of H_2 desorption profiles at different temperatures for the solid-state 4-K-pip dehydrogenation catalyzed by 5 % Rh/C

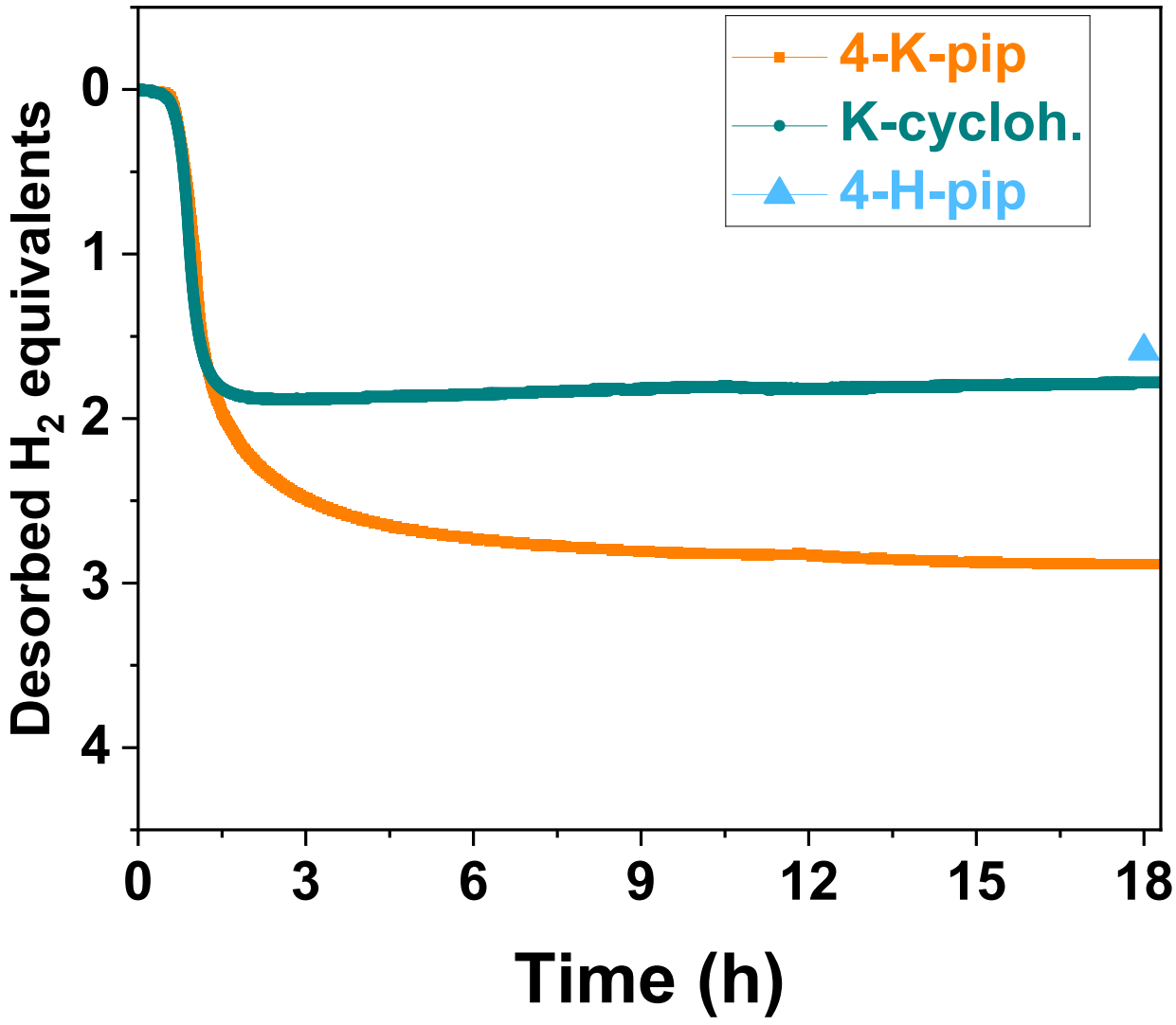

Fig. S9. Comparison of H_2 desorption performance between 4-K-pip, 4-H-pip, and K-cyloh; catalyzed by 5% Rh/C from room temperature to 120 °C. 4-H-pip could not be tested using the HPSA-auto Pro gas adsorption analyzer due to its boiling and melting points, which are lower than the reaction temperature. Thus, while the H_2 equivalents desorbed from 4-K-pip and K-cyloh were calculated from the experimental desorbed H_2 capacity, the H_2 equivalents desorbed from 4-H-pip were calculated from the substrate conversion determined from the ^{1}H NMR spectrum of the post-H_2 desorption sample.

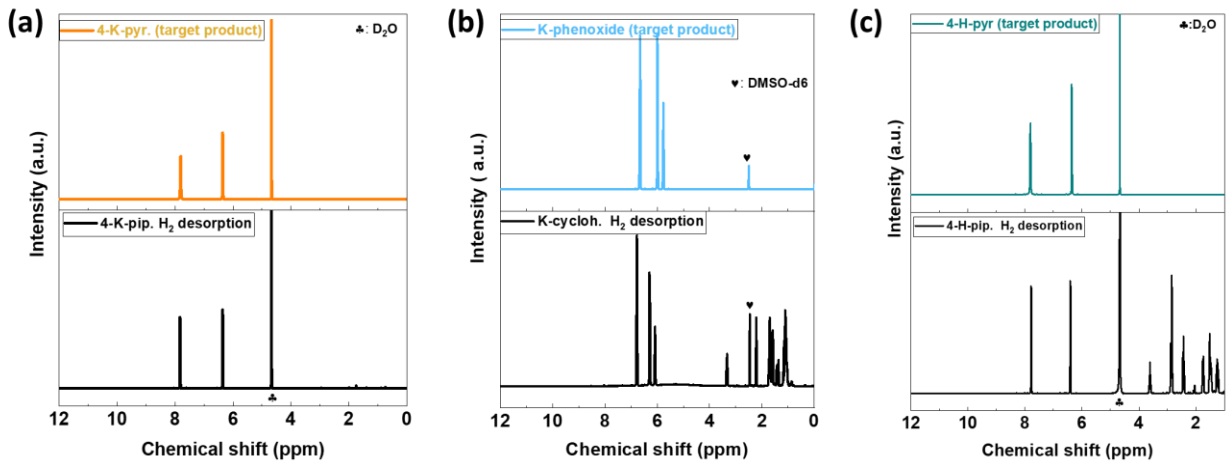

Fig. S10. ^{1}H NMR spectra of post-H_2 desorption sample for 4 K-pip (**a**), K-cycloh (**b**), and 4 H-pip (**c**). Catalyst: 5% Rh/C, temperature: RT-120 °C, substrate-to-Rh molar ratio: 5/1. Spectra of post-H_2 desorption samples are compared to those of the substrates and the target products to demonstrate the reaction selectivity.

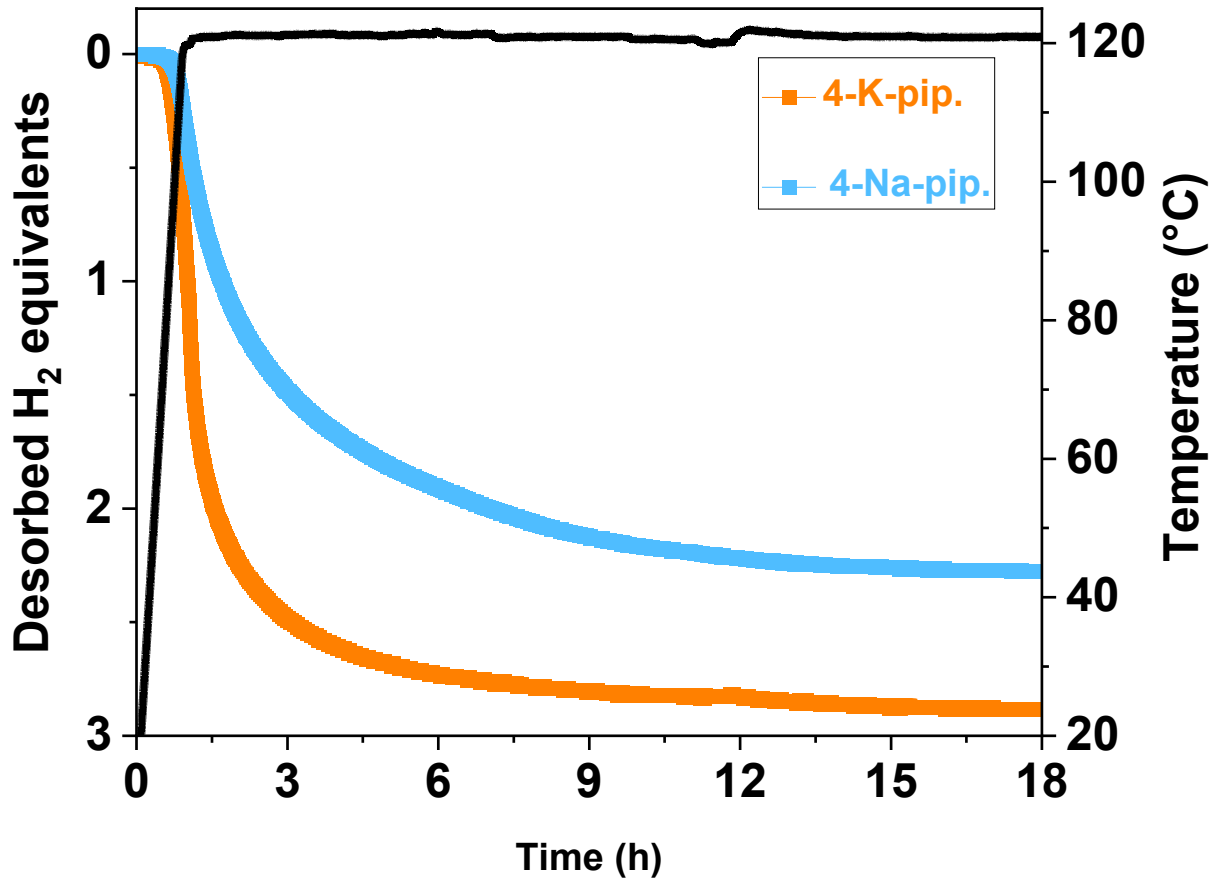

Fig. S11. Comparison of H_2 desorption performance between 4-K-pip and 4-Na-pip**.** Catalyst: 5% Rh/C, temperature: RT-120 °C, substrate-to-Rh molar ratio: 5/1.

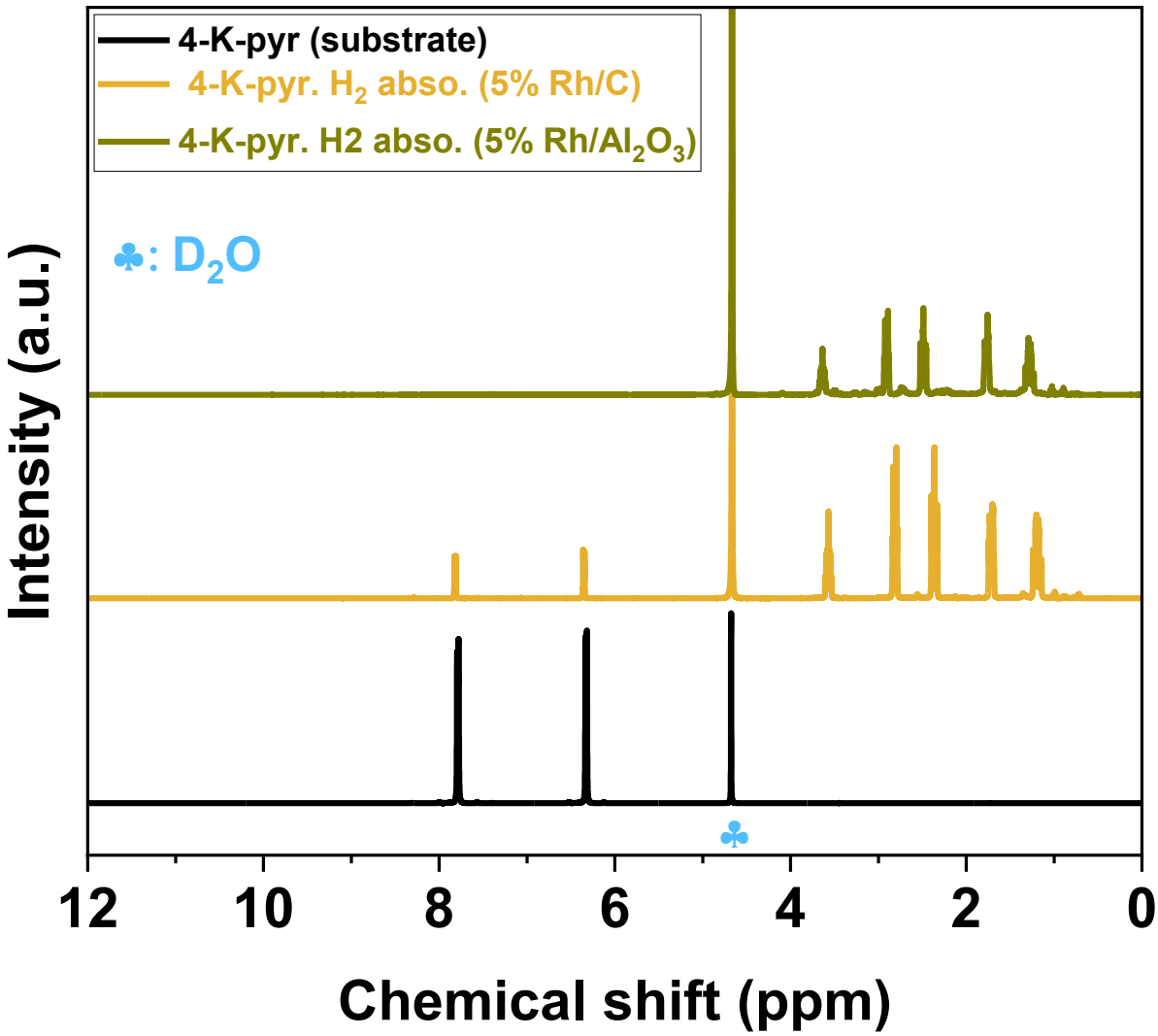

Fig. S12. ^{1}H NMR characterization of samples recovered from solid-state hydrogenation of 4-K-pyr catalyzed by 5% Rh/C and 5% Rh/Al_2O_3 under 60 bar H_2 pressure, substrate-to-metal molar ratio: 2/1, temperature: 120 °C.

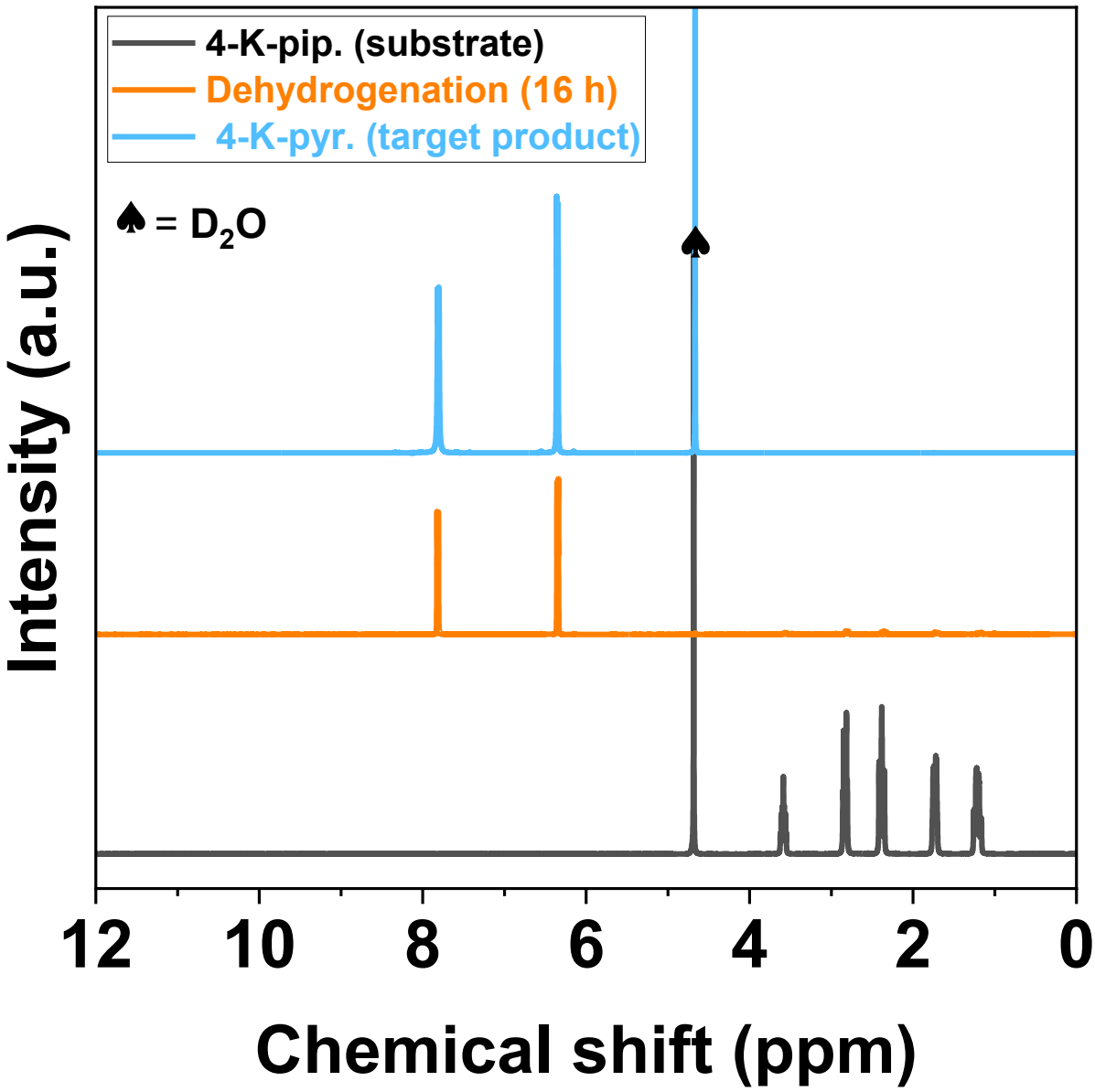

Fig. S13. ^{1}H NMR characterization of a sample recovered from 4-K-pip dehydrogenation in aqueous solution catalyzed by 5% Rh/C at 100 °C. The spectrum of the 4-K-pip post-dehydrogenation sample is compared to those of the substrate and the target product to demonstrate the excellent reaction conversion and selectivity.

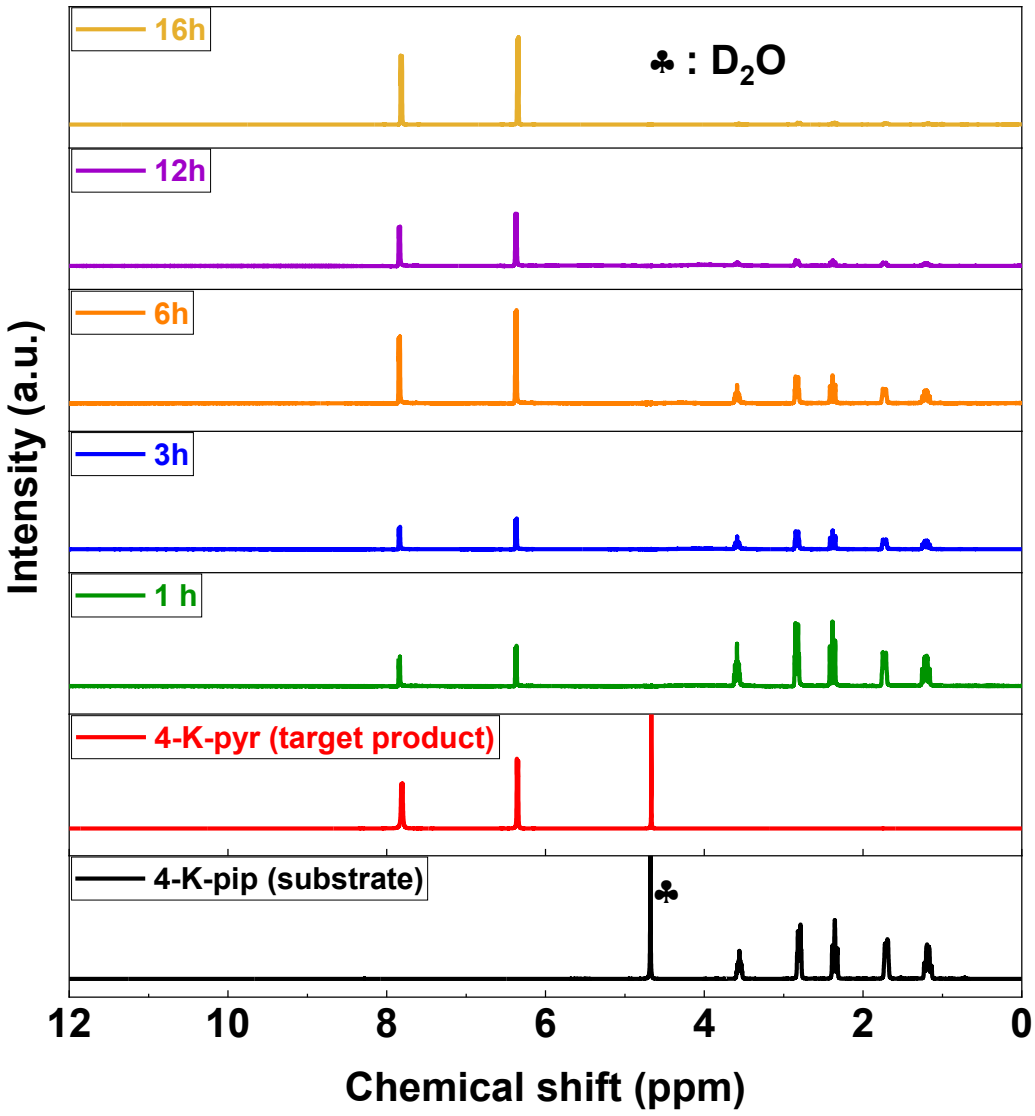

Fig. S14. ^{1}H NMR spectra of samples taken at different time intervals during the dehydrogenation of 4 K-pip in aqueous solution catalyzed by 5% Rh/C at 100 °C. These spectra are compared to those of the substrate and the target product to demonstrate the excellent reaction conversion and selectivity.

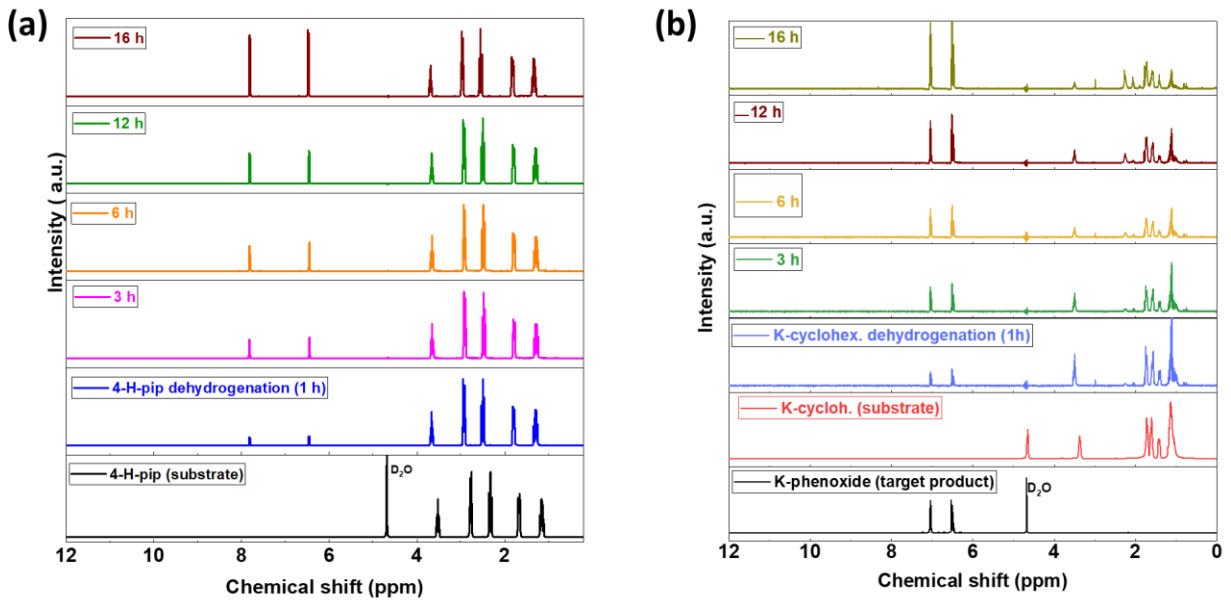

Fig. S15. ^{1}H NMR spectra of samples taken at different time intervals during the dehydrogenation of 4-H-pip (a) and K-cycloh (b) in aqueous solution. Catalyst: 5% Rh/C, temperature: 100 °C. These spectra are compared to those of the substrate and the target product to demonstrate the reaction conversion and selectivity.

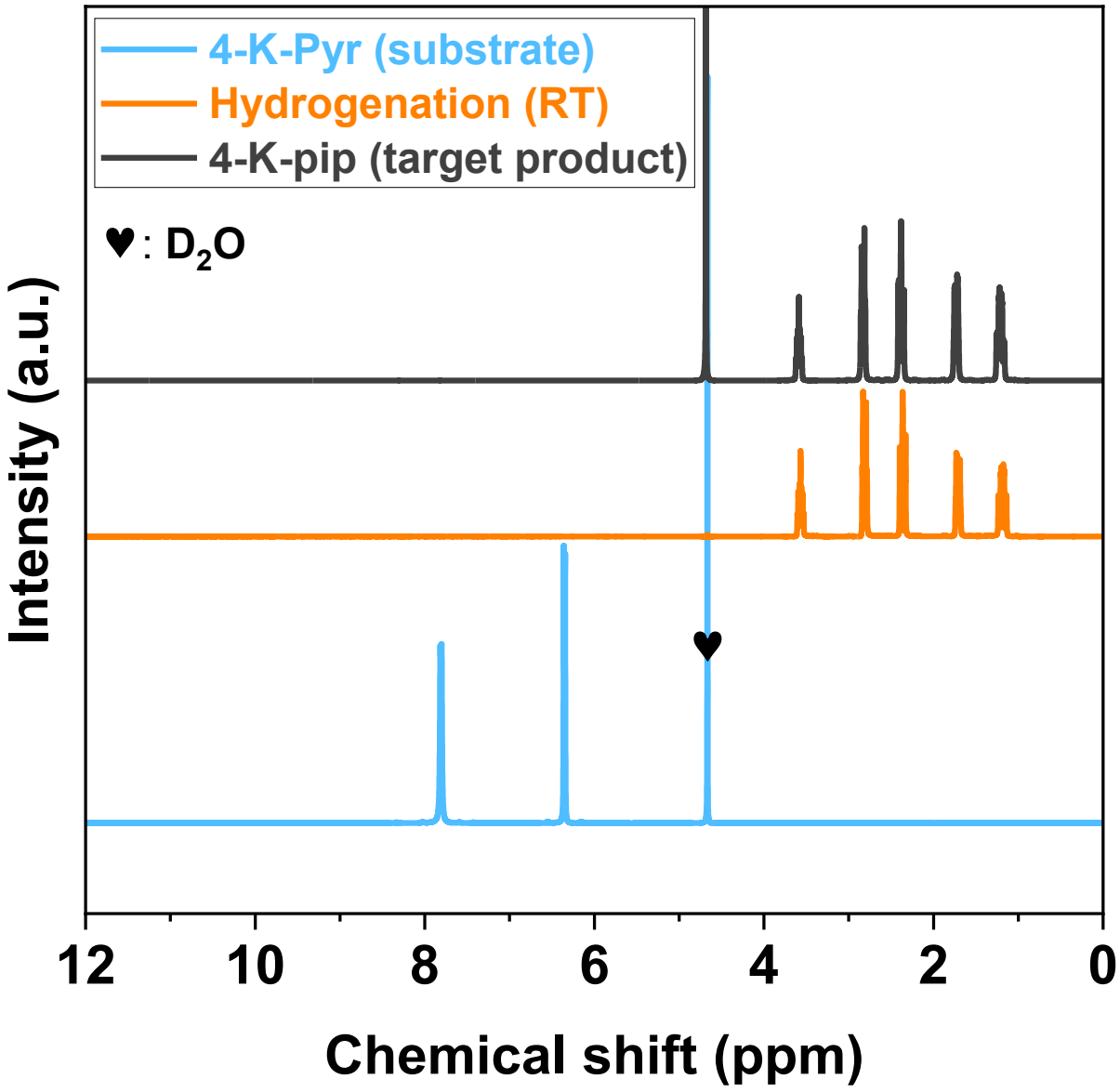

Fig. S16. ^{1}H NMR spectrum of 4-K-pyr post-hydrogenation sample. Catalyst: 5% Rh/C, substrate-to-Rh molar ratio: 30/1, pressure: 40 bar H_2, room temperature (RT). This spectrum is compared to those of the substrate and the target product to demonstrate the excellent reaction conversion and selectivity.

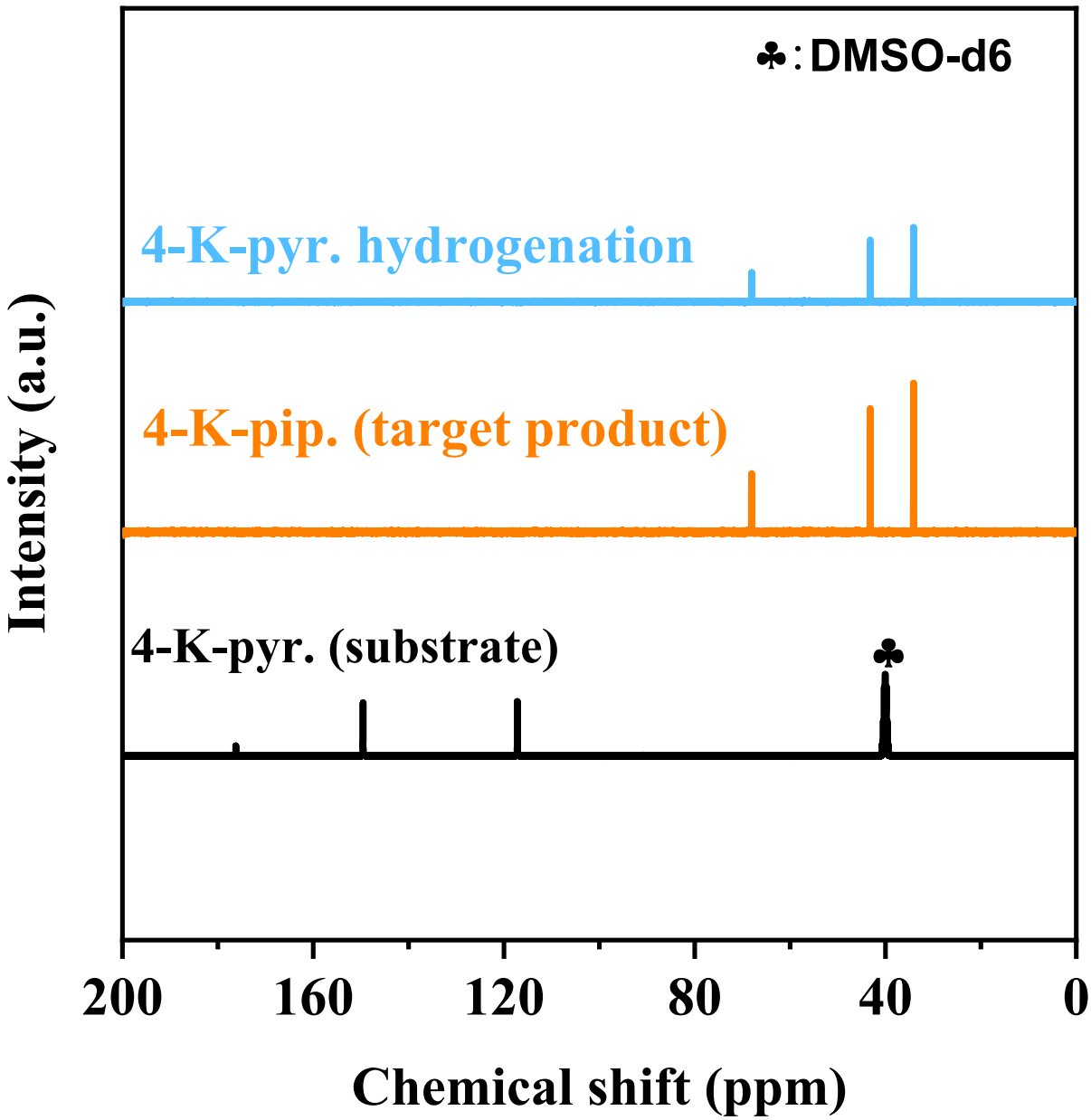

Fig. S17. ^{13}C NMR spectrum of 4-K-pyr post-hydrogenation sample. Catalyst: 5% Rh/C, substrate-to-Rh molar ratio: 30/1, pressure: 40 bar H_2, room temperature (RT). This spectrum is compared to those of the substrate and the target product to demonstrate the excellent reaction conversion and selectivity.

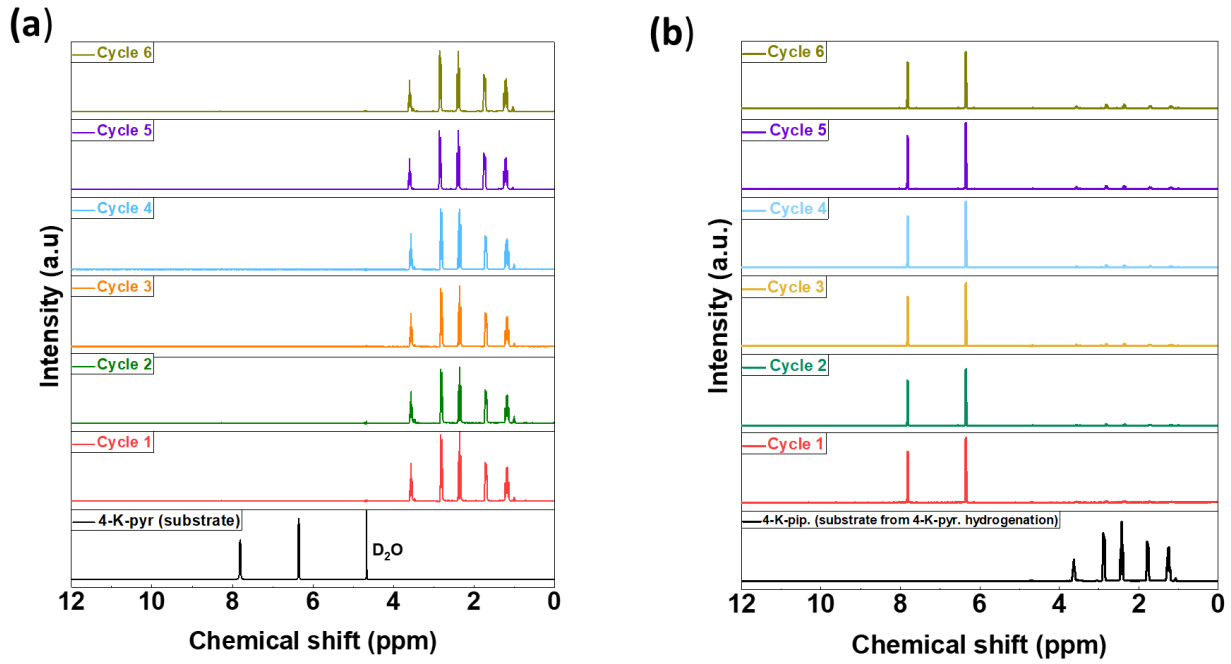

Fig. S18. ^{1}H NMR Spectra of samples taken after every hydrogenation process (a) and dehydrogenation process (b) during the cycling stability test of the 4-K-pip/4-K-pyr pair in aqueous solution at 100 °C using 5% Rh/C as a bidirectional catalyst. Catalyst: 5% Rh/C, substrate-to-Rh molar ratio: (20/1), hydrogenation pressure: 40 bar H_2, hydrogenation time: 3 h, dehydrogenation time: 16 h.

Table S1. Comparison of the K-4-piperidinolate/4-pyridinolate pair with other hydrogen storage

H_2 storage systems	**ΔH_d (kJ/mol-H_2)**	**T_d (°C)**	**HSC (wt%)**	**Air stability**	**Reversibility**	**Material Cost†**	**Ref.**
Potassium 4-piperidinolate/4-pyridinolate (4-K-pip/4-K-pyr)	35.2	100-120	4.3	Yes	High	Low	This work
Methylcyclohexane/toluene (MCH/TOL)	68.3	>300	6.2	Yes	High	Low	[5, 6]
Perhydrodibenzyltoluene/Dibenzyltoluene (H12-DBT/H0-DBT)	65.4	310	6.2	Yes	High	Moderate	[6, 7]
Dodecahydro-N-ethylcarbazole/ N-ethylcarbazole (H12-NEC/NEC)	50.6	180	5.8	Yes	High	Moderate	[6, 8]
Formic acid/CO_2	31.2 (salt)	100	4.4	Yes	Circular*	Low	[6, 9]
Methanol + H_2O/CO_2	16.6	>200	12.1	Yes	Circular*	Low	[10, 11]
NH_3/N_2	30.7	300-500	17.8	-	Circular*	Low	[12, 13]
Sodium cyclohexanolate/phenoxide	50.4	100-140	4.9	Yes	High	Low	[14]
MgH_2/Mg	76.0	300	7.6	No	High	High	[15]
$LiBH_4$/LiH + B	74.0	>370	13.8	No	Low	High	[16]
$NaAlH_4$/NaH + Al	53.0	>200	5.5	No	Limited	High	[17]
$LaNi_5H_x$/$LaNi_5$	31.7	<100	1.5	Yes	High	High	[18]

*A circular hydrogen carrier releases H_2 together with a co-product, such as CO_2 or N_2, as its H-lean format. The regeneration of the carrier requires the recapture and reutilization of the gaseous co-product, or its supply from an external source, thereby enabling a closed and recyclable hydrogen storage–release cycle rather than a one-way feedstock route [19].

†*Low*: commodity (bulk) materials or raw materials, *moderate*: commercial materials, *high*: specialty chemicals

References

1. J. Wu, I. Ying Zhang and X. Xu, *ChemPhysChem*, 2010, **11**, 2561-2567.
2. M. J. Trucks, G. W. Schlegel, H. B. Scuseria, et al., Gaussian˜16 Revision C .01. 2016.
3. A. C. Larson, R. B. Dreele and B. Toby, 1994, **748**.
4. R. E. Dinnebier, M. Pink, J. Sieler and P. W. Stephens, *Inorganic Chemistry*, 1997, **36**, 3398-3401.
5. P. T. Aakko-Saksa, C. Cook, J. Kiviaho and T. Repo, *Journal of Power Sources*, 2018, **396**, 803-823.
6. M. Niermann, S. Drünert, M. Kaltschmitt and K. Bonhoff, *Energy & Environmental Science*, 2019, **12**, 290-307.
7. H. Jorschick, P. Preuster, S. Dürr, A. Seidel, K. Müller, A. Bösmann and P. Wasserscheid, *Energy & Environmental Science*, 2017, **10**, 1652-1659.
8. B. Wang, P.-y. Li, S.-y. Wang, S.-h. Lu and T. Fang, *ACS Sustainable Chemistry & Engineering*, 2023, **11**, 5485-5494.
9. J. Eppinger and K.-W. Huang, *ACS Energy Letters*, 2017, **2**, 188-195.
10. S. Sá, H. Silva, L. Brandão, J. M. Sousa and A. Mendes, *Applied Catalysis B: Environmental*, 2010, **99**, 43-57.
11. J. Kothandaraman, S. Kar, R. Sen, A. Goeppert, G. A. Olah and G. K. S. Prakash, *Journal of the American Chemical Society*, 2017, **139**, 2549-2552.
12. I. Lucentini, X. Garcia, X. Vendrell and J. Llorca, *Industrial & Engineering Chemistry Research*, 2021, **60**, 18560-18611.
13. E. Spatolisano, L. A. Pellegrini, A. R. de Angelis, S. Cattaneo and E. Roccaro, *Industrial & Engineering Chemistry Research*, 2023, **62**, 10813-10827.
14. Y. Yu, T. He, A. Wu, Q. Pei, A. Karkamkar, T. Autrey and P. Chen, *Angewandte Chemie International Edition*, 2019, **58**, 3102-3107.
15. V. A. Yartys, M. V. Lototskyy, E. Akiba, R. Albert, V. E. Antonov, J. R. Ares, M. Baricco, N. Bourgeois, C. E. Buckley, J. M. Bellosta von Colbe, J. C. Crivello, F. Cuevas, R. V. Denys, M. Dornheim, M. Felderhoff, D. M. Grant, B. C. Hauback, T. D. Humphries, I. Jacob, T. R. Jensen, P. E. de Jongh, J. M. Joubert, M. A. Kuzovnikov, M. Latroche, M. Paskevicius, L. Pasquini, L. Popilevsky, V. M. Skripnyuk, E. Rabkin, M. V. Sofianos, A. Stuart, G. Walker, H. Wang, C. J. Webb and M. Zhu, *International Journal of Hydrogen Energy*, 2019, **44**, 7809-7859.
16. A. Züttel, P. Wenger, S. Rentsch, P. Sudan, P. Mauron and C. Emmenegger, *Journal of Power Sources*, 2003, **118**, 1-7.
17. B. Bogdanović, R. A. Brand, A. Marjanović, M. Schwickardi and J. Tölle, *Journal of Alloys and Compounds*, 2000, **302**, 36-58.
18. S. Sleiman, S. Shahgaldi and J. Huot, *Journal*, 2024, **5**, 419-428.
19. Z. Abdin, C. Tang, Y. Liu and K. Catchpole, *iScience*, 2021, **24**, 102966.